



A Computational Model of Dual Competition between the Basal Ganglia and the Cortex

Meropi Topalidou, Daisuke Kase, Thomas Boraud, Nicolas P. Rougier

► To cite this version:

Meropi Topalidou, Daisuke Kase, Thomas Boraud, Nicolas P. Rougier. A Computational Model of Dual Competition between the Basal Ganglia and the Cortex. *eNeuro*, 2018, pp.ENEURO.0339-17.2018. hal-01925643

HAL Id: hal-01925643

<https://inria.hal.science/hal-01925643>

Submitted on 16 Nov 2018

HAL is a multi-disciplinary open access archive for the deposit and dissemination of scientific research documents, whether they are published or not. The documents may come from teaching and research institutions in France or abroad, or from public or private research centers.

L'archive ouverte pluridisciplinaire **HAL**, est destinée au dépôt et à la diffusion de documents scientifiques de niveau recherche, publiés ou non, émanant des établissements d'enseignement et de recherche français ou étrangers, des laboratoires publics ou privés.

A Computational Model of Dual Competition between the Basal Ganglia and the Cortex

Meropi Topalidou,^{1,2,3,4,†} Daisuke Kase,^{2,3,5,†} Thomas Boraud,^{2,3,5,6,‡} and Nicolas P. Rougier^{1,2,3,4,‡,*}

¹INRIA Bordeaux Sud-Ouest 33405 Talence, France ²Institut des Maladies Neurodégénératives, Université de Bordeaux, 33000, Bordeaux, France ³Institut des Maladies Neurodégénératives, CNRS, UMR 5293, 33000, Bordeaux, France ⁴LaBRI, Université de Bordeaux, Institut Polytechnique de Bordeaux, CNRS, UMR 5800, 33405 Talence, France ⁵CNRS, French-Israeli Neuroscience Lab, 33000 Bordeaux, France ⁶CHU de Bordeaux, Institut MN Clinique, 33000 Bordeaux, France [†]These authors have contributed equally to this work. [‡]These authors have also contributed equally to this work.

*Corresponding author: Nicolas.Rougier@inria.fr

Abstract. We propose a model that includes interactions between the cortex, the basal ganglia and the thalamus based on a dual competition. We hypothesize that the striatum, the subthalamic nucleus, the internal pallidum (GPI), the thalamus, and the cortex are involved in closed feedback loops through the hyperdirect and direct pathways. These loops support a competition process that results in the ability of basal ganglia to make a cognitive decision followed by a motor one. Considering lateral cortical interactions, another competition takes place inside the cortex allowing the latter to make a cognitive and a motor decision. We show how this dual competition endows the model with two regimes. One is driven by reinforcement learning, the other by Hebbian learning. The final decision is made according to a combination of these two mechanisms with a gradual transfer from the former to the latter. We confirmed these theoretical results on primates (*Macaca mulata*) using a novel paradigm predicted by the model.

Significance statement. In this article, we propose a detailed computational model of interaction between basal ganglia and cortex in which, the former adapts its response according to the outcome while the latter is insensitive to it. The model shows how these two processes interact in order to issue a unique behavioral answer. This prediction has been verified on monkeys, demonstrating how these two processes are both competing (expression) and cooperating (learning). These results suggest that a behavioral decision emerges actually from a dual competition of two distinct but entangled systems.

Keywords: Cortex, Basal Ganglia, Thalamus, Reinforcement Learning, Hebbian Learning, Covert Learning, Stimulus-Response, Action-Outcome, Decision making, Action Selection, Competition, Short-range Excitation, Long-range Inhibition

Document statistics

Abstract: 159 words

Significance Statement: 88 words

Introduction: 891 words

Discussion: 1046 words

Introduction

Action-outcome (A-O) and stimulus-response (S-R) processes, two forms of instrumental conditioning, are important components of behavior. The former evaluates the benefit of an action in order to choose the best one among those available (action selection), while the latter is responsible for automatic behavior (routines), eliciting a response as soon as a known stimulus is presented (Graybiel, 2008; Mishkin, Malamut, & Bachevalier, 1984), independently of the hedonic value of the stimulus. Action selection can be easily characterized by using a simple operant conditioning setup, such as a two-armed bandit task, where an animal must choose between two options of different value, the value being probability, magnitude or quality of reward (Guthrie, Leblois, Garenne, & Boraud, 2013; Pasquereau et al., 2007). After some trial and error, a wide variety of vertebrates are able to select the best option (Bradshaw, Szabadi, Bevan, & Ruddle, 1979; Dougan, McSweeney, & Farmer, 1985; Gilbert-Norton, Shahan, & Shivik, 2009; Graft, Lea, & Whitworth, 1977; Herrnstein, 1974; Herrnstein, Vaughan, Mumford, & Kosslyn, 1989; Lau & Glimcher, 2005, 2008; Matthews & Temple, 1979). After intensive training, which depends on the species and the task and whether the same values are used throughout the series of the experiments, the animal will tend to become insensitive to change and persist in selecting the formerly best option (Lau & Glimcher, 2005; Yin & Knowlton, 2006). Most of the studies on action selection and habits/routines agree on a slow and incremental transfer from the action-outcome to the stimulus-response system such that after extensive training, the S-R system takes control of behavior and the animal becomes insensitive to reward devaluation (Packard & Knowlton, 2002; Seger & Spiering, 2011). Oddly enough, very little is known on the exact mechanism underlying such transfer. One difficult question that immediately arises is when and how the brain switches from a flexible action selection system to a more static one.

Our working hypothesis is that there is no need for such an explicit switch. We propose instead that an action expressed in the motor area results from both the continuous cooperation (acquisition) and competition (expression) of the two systems. To do so, we consider the now classical actor-critic model of decision making elaborated in the 1980s which posits that there are two separate components in order to explicitly represent the policy independently from the value function. The actor is in charge of choosing an action in a given state (policy), while the critic is in charge of evaluating (criticizing) the current state (value function). This classical view has been used extensively for modeling the basal ganglia (Doll, Bradley B, Simon, Dylan A, & Daw, Nathaniel D, 2012; Doya, 2007; Frank, 2004; Glimcher, 2011; Suri, R E & Schultz, W, 1999; Suri, 2002), even though the precise anatomical mapping of these two processes is still subject to debate and may diverge from one model to the other (Niv, Yael & Langdon, Angela, 2016; Redgrave, Peter, Gurney, Kevin, & Reynolds, John, 2008). However, all these models share the implicit assumption that the actor and the critic are interacting, i.e. the actor determines the policy exclusively from the values estimated by the critic, as in Q-Learning or SARSA. Interestingly enough, Sutton, R S and Barto, A G (1998) noted in their seminal work that one could imagine intermediate architectures in which both an action-value function and an independent policy would be learned.

We support this latter hypothesis based on a decision-making model that is grounded on anatomical and physiological data and that identify the cortex-basal ganglia (CBG) loop as the actor. The critic of which the Substantia Nigra pars compacta (SNc) and the Ventral Tegmental Area (VTA) are essential components interacts through dopamine projections to the striatum (Leblois, Boraud, Meissner, Bergman, & Hansel, 2006). Decision is generated by symmetry breaking mechanism that emerges from competitions processes between positives and negatives feedback loop encompassing the full CBG network (Guthrie et al., 2013). This model captured faithfully

behavioural, electrophysiological and pharmacological data we obtained in primates using implicit variant of two-armed bandit tasks – that assessed both learning and decision making – but was less consistent with the explicit version (i.e. when values are known from the beginning of the task) that focus on the decision process only.

We therefore modified this early model by adding a cortical module that has been granted with a competition mechanism and Hebbian learning (Doya, 2000). This improved version of the model predicts that the whole CBG loop is actually necessary for the implicit version of the task, however, when the basal ganglia feedback to the cortex is disconnected, the system is nonetheless able to make a decision in the explicit version of the task. Our experimental data fully confirmed this prediction (Piron et al., 2016) and allowed us to solve an old conundrum concerning the pathophysiology of the BG: a lesion or jamming of the output of the BG improve Parkinson patient motor symptoms while it affects marginally their cognitive and psycho-motor performances.

An interesting prediction of this generalized actor-critic architecture is that the valuation of options and the behavioral outcome are segregated. In the computational model, it's implied that if we block the output of the basal ganglia in a two-armed bandit task before learning, this should induce covert learning during the random choices of the model, because reinforcement learning should still occur at the striatal level under dopaminergic control. The goal of this study is thus twofold: i) to present a comprehensive description of the model in order to provide the framework for an experimental paradigm that allows to disclose covert learning and ii) to test this prediction in monkeys.

Materials and Methods

The task

We consider a variant of a n -armed bandit task (Auer, Cesa-Bianchi, Freund, & Schapire, 2002; Katehakis & Veinott, 1987) where a player must decide which arm of n slot machines to play in a finite sequence of trials to maximize his accumulated reward. This task has received much attention in the literature (e.g. machine learning, psychology, biology, game theory, economics, neuroscience, etc.), because it provides a simple model to explore the trade-off between exploration (trying out a new arm to collect information about its payoff) and exploitation (playing the arm with the highest expected payoff) (Gittins, 1979; Robbins, 1952). This task has been shown to be solvable for a large number of different living beings, with (Kearar, 2002; Plowright & Shettleworth, 1990; Steyvers, Lee, & Wagenmakers, 2009) or without a brain (Reid et al., 2016), and even a clever physical apparatus can solve the task (Naruse et al., 2015).

The computational task

In the present study, we restrict the n -armed bandit task to $n = 2$ with an explicit dissociation between the choice of the option (*cognitive* choice) and the actual triggering of the option (*motor* choice). This introduces a supplementary difficulty because only the motor choice – the physical (and visible) expression of the choice – will be taken into account when computing the reward. If cognitive and motor choices are incongruent, only the motor choices matters. Unless specified otherwise, we consider a set of cues $\{C_i\}_{i \in [1, n]}$ associated with reward probabilities $\{P_i\}_{i \in [1, n]}$ and a set of four different locations ($\{L_i\}_{i \in [1, 4]}$) corresponding to the *up*, *down*, *left*, *right* positions on the screen. A trial is made of the presentation of two random cues C_i and C_j ($i \neq j$) at two random locations (L_i and L_j) such that we have $L_i \neq L_j$ (see Fig. 1). A session is made of n successive trials and can use one to several different cue sets depending on the condition studied (e.g. reversal, devaluation). Unless specified otherwise, in the present study, exactly one cue set is

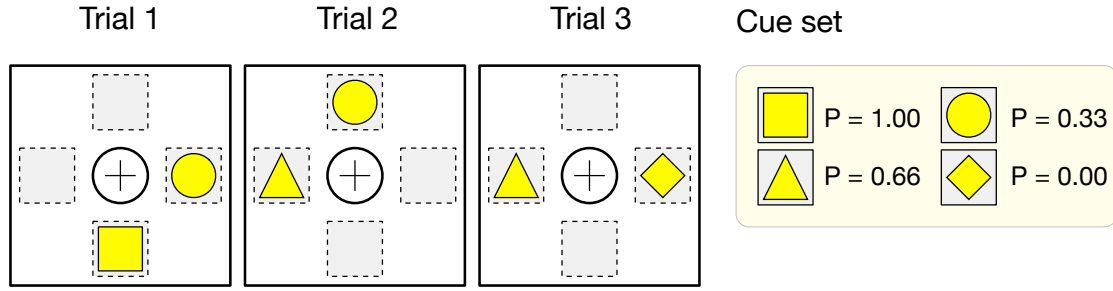


Figure 1. Three task trials from a 4-items cue set (\square , \triangle , \circ , \diamond) with respective reward probabilities (1, 0.33, 0.66 and 0).

used throughout a whole session.

Once a legal motor decision has been made (i.e. a motor action corresponding to one of the stimulus position), the reward is computed by drawing a random uniform number between 0 and 1. If the number is less or equal to the reward probability of the chosen cue, a reward of 1 is given, otherwise, a reward of 0 is given. If no motor choice has been made or if the motor choice leads to an empty location (illegal choice), the trial is considered to be failed and no reward is given, which is different from giving a reward of 0. The best choice for a trial is defined as the choice of the cue associated with the highest reward probability among the two presented cues. Performance is defined as the ratio of best choices over the total number of trials. A perfect player with full-knowledge can achieve a performance of 1 while the mean expectation of the reward is directly dependent on the cue sampling policy. For example on Fig. 1, if we consider a uniform cue sampling policy for $6 \times n$ trials, the mean expected reward for a perfect player with full knowledge is $\frac{3}{6} \times 1 + \frac{2}{6} \times \frac{2}{3} + \frac{1}{6} \times \frac{1}{3} = \frac{14}{18} \approx 0.777\dots$.

The behavioral task

With kind permission from the authors (Piron et al., 2016), we reproduce here the details of the experimental task which is similar.

The primates were trained daily in the experimental room and familiarized with the setup, which consisted of 4 buttons placed on a board at different locations (0° , 90° , 180° , and 270°), and a further button in a central position, which detects contact with a monkey's hand. These buttons correspond to the 4 possible display positions of a cursor on a vertical screen. The monkeys were seated in chairs in front of this screen at a distance of 50cm (Fig. 2). The monkeys initiated a trial by keeping their hands on the central button, which induced the appearance of the cursor in the central position of the screen. After a random delay (0.5s to 1.5s), 2 cues appeared in 2 (of 4) different positions determined randomly for each trial. Each cue had a fixed probability of reward ($P_1 = 0.75$ and $P_2 = 0.25$) and remains the same during a session. Once the cues were shown, the monkeys had a random duration time window (0.5s to 1.5s) to press the button associated with one cue. It moves the cursor over the chosen cue and they have to maintain the position for 0.5 s to 1.5 s. After this delay, the monkeys were rewarded (0.3 ml of water) or not according to the reward probability of the chosen target. The disappearance of the cursor corresponds to an end-of-trial signal, indicating to the monkeys that the trial was finished and they could start a new trial after an inter-trial interval between 0.5 s and 1.5s.

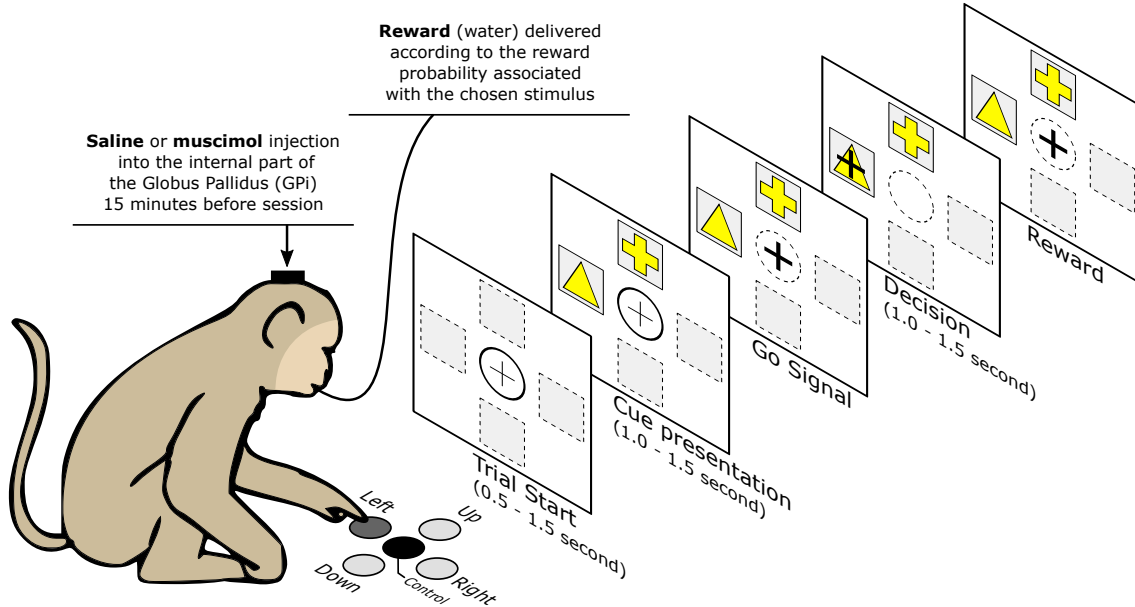


Figure 2. The behavioral task. The monkeys initiate a trial by keeping their hands on the central button, which induced the appearance of the cursor in the central position of the screen. After a random delay, two cues appears in 2 different positions. The monkey has a random duration time window (0.5s to 1.5s) to press the button associated with one cue. It moves the cursor over the chosen cue and has to maintain the position for some duration. After this delay, the monkey is rewarded (0.3 ml of water) or not according to the reward probability of the chosen cue.

The model

The model is designed to study the implications of a dual competition between the cortex and the basal ganglia (BG). It is segregated into three territories partially overlapping at the striatal level (for full discussion see (Guthrie et al., 2013)). The motor territory elicits the actual behavioral choice of the model by selecting one of the two positions in which the cues are presented. It roughly corresponds to the supplementary motor area and associated sub-cortical territories. The cognitive loop chooses one of the two cues that are displayed roughly corresponding to the role devoted to the dorsal lateral prefrontal cortex and associated sub-territories. The associative cortex provide a contextual map indicating which cue is presented where on each trial and roughly correspond to the parietal cortex. While in the animal we have access only to the actual choice (provided by the actual behavior of the animal), the model allowed us to have access to the internal choice by looking at which of the two cues was selected at each trial. It could happen that the *cognitive* loop chooses one cue, while the *motor* loop chooses the position of the other one, especially at the beginning of the trial, when the synaptic signal to noise is still weak due to low gain. This cognitive dissonance maybe a mechanism for impulsivity, but it is beyond the scope of this paper.

The competition inside the cortex is conveyed through direct lateral interactions using short-range excitation and long range inhibition (Coultrip, Granger, & Lynch, 1992; Deco et al., 2014; Muir & Cook, 2014; H. R. Wilson & Cowan, 1972, 1973)), while the competition within the BG is conveyed through the direct and hyperdirect pathways (Guthrie et al., 2013; Leblois et al., 2006). Therefore, the indirect pathway and the external segment of the globus pallidus (GPe) are not included. In order to solve the task, the model relies on the competition between diverging negative feedback loops that provide lateral inhibition, and parallel positive feedback loops that promote differential activation allowing the issue of different cognitive and motor choices. This

competitive mechanism occurs at both the basal and cortical level, but the final decision is derived from the cortical level. As soon as the motor cortex activity is above a given threshold, the model is considered to have made a decision. In contrast to (Doya, 2007; Frank, 2004; Gurney, Prescott, & Redgrave, 2001), our model relies heavily on feedback mechanisms and closed loops while the latter are purely feed-forward models that merely answer to inputs.

Architecture

Our model contains five main groups. Three of these groups are excitatory: the cortex (CTX), the thalamus (THL), and the subthalamic nucleus (STN). Two populations are inhibitory corresponding to the sensorymotor territories of the striatum (STR) and the GPi. The model has been further tailored into three segregated loops (Alexander & Crutcher, 1990; Alexander, Crutcher, & DeLong, 1991; Alexander, DeLong, & Strick, 1986; Haber, 2003; Mink, 1996), namely the motor loop, the associative loop and the cognitive (or limbic) loop. The motor loop comprises the motor cortex (supplementary motor area, primary cortex, premotor cortex, cingulate motor area), the motor striatum (putamen), the motor STN, the motor GPi (motor territory of the pallidum and the substantia nigra) and the motor thalamus (ventrolateral thalamus). The associative loop comprises the associative cortex (dorsolateral prefrontal cortex, the lateral orbitofrontal cortex) and the associative striatum (associative territory of the caudate). The cognitive loop comprises the cognitive cortex (anterior cingulate area, medial orbitofrontal cortex), the cognitive striatum (ventral caudate), the cognitive STN, the cognitive GPi (limbic territory of the pallidum and the substantia nigra), and the cognitive thalamus (ventral anterior thalamus).

Populations

The model consists of 12 populations: 5 motor, 4 cognitive and 2 associative populations (Fig. 3). These populations comprise from 4 to 16 neural assemblies and each possesses a specific geometry whose goal is to facilitate connectivity description. Each assembly is modeled using a neuronal rate model (Hopfield, 1984; Shriki, Hansel, & Sompolinsky, 2003) that give account of the spatial mean firing rate of the neurons composing the assembly. Each assembly is governed by the following equations:

$$\tau \frac{dV}{dt} = -V + I_{syn} + I_{ext} + h \quad (1)$$

$$U = f(V + V.n) \quad (2)$$

where τ is the assembly time constant (decay of the synaptic input), V is the firing rate of the assembly, I_{syn} is the synaptic input to the assembly, I_{ext} is the external input representing the sensory visual salience of the cue, h is the threshold of the assembly, f is the transfer function and n is the (correlated, white) noise term. Each population possess its own set of parameters according to the group it belongs to (see Table 1). Transfer function for all population but the striatal population is a ramp function ($f(x) = \max(x, 0)$). The striatal population that is silent at rest (Sandstrom & Rebec, 2002), requires concerted coordinated input to cause firing (C. J. Wilson & Groves, 1981), and has a sigmoidal transfer function (nonlinear relationship between input current and membrane potential) due to both inward and outward potassium current rectification (Nisenbaum & Wilson, 1995). This is modeled by applying a sigmoidal transfer function to the activation of cortico-striatal inputs in the form of the Boltzmann equation:

$$f(x) = V_{min} + \frac{V_{max} - V_{min}}{1 + e^{-\frac{V_h - x}{V_c}}}$$

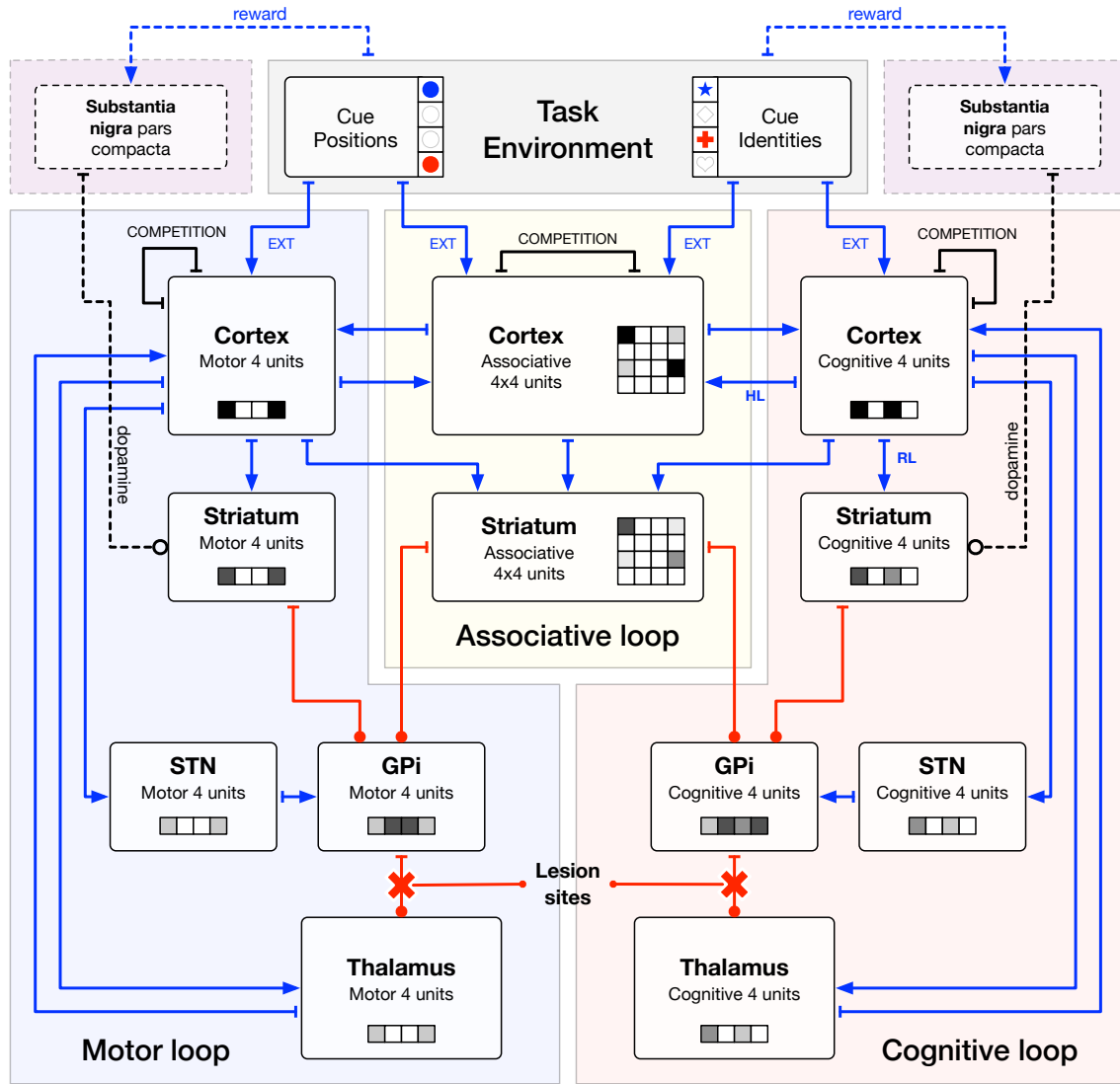


Figure 3. Architecture of the model. The architecture of the model is centered around the hyperdirect pathway (cortex → subthalamic nucleus → GPi/SNR → thalamus → cortex), the direct pathway (cortex → striatum → GPi/SNR → thalamus → cortex) and the cortex where lateral interactions take place. The model is further detailed into three segregated circuits (cognitive, associative, motor). The cognitive and motor circuit each comprises a cortical, a striatal, a thalamic, a subthalamic, and a pallidal population while the associative loop only comprises a cortical and a striatal population. This latter interacts with the two other circuits via diffused connections to the pallidal regions and from all cortical populations. Arrows, excitatory connections. Dots, inhibitory connections.

Population		Geometry	τ	Threshold	Noise
Cortex	associative	(4,4)	10ms	-3	1.0%
	cognitive	(4,1)	10ms	-3	1.0%
	motor	(1,4)	10ms	-3	1.0%
Striatum	associative	(4,4)	10ms	0	0.1%
	cognitive	(4,1)	10ms	0	0.1%
	motor	(4,1)	10ms	0	0.1%
GPi	cognitive	(4,1)	10ms	-10	3.0%
	motor	(1,4)	10ms	-10	3.0%
STN	cognitive	(4,1)	10ms	-10	0.1%
	motor	(1,4)	10ms	-10	0.1%
Thalamus	cognitive	(4,1)	10ms	-40	0.1%
	motor	(1,4)	10ms	-40	0.1%

Table 1. Population parameters

Name	Value
V_{min}	1
V_{max}	20
V_h	16
V_c	3

Table 2. Parameters for striatal sigmoid transfer function

where V_{min} is the minimum activation, V_{max} the maximum activation, V_h the half- activation, and V_c the slope. This is similar to the use of the output threshold in the (Gurney et al., 2001) model and results in small or no activation to weak inputs with a rapid rise in activation to a plateau level for stronger inputs. The parameters used for this transfer function are shown in Table 2 and were selected to give a low striatal output with no cortical activation (1 spike/s), starting to rise with a cortical input of 10 sp/s and a striatal output of 20 spike/s at a cortical activation of 30 spike/s.

Connectivity

Even though the model takes advantage of segregated loops, they cannot be entirely separated if we want the cognitive and the motor channel to interact. This is the reason why we incorporated a divergence in the cortico-striatal connection followed by a re-convergence within the GPi (Graybiel, Aosaki, Flaherty, & Kimura, 1994; Parent et al., 2000) (see Fig. 4). Furthermore, we considered the somatotopic projection of the pyramidal cortical neurons to the striatum (Webster, 1961) as well as their arborization (Cowan & Wilson, 1994; Parent et al., 2000; Parthasarathy, Schall, & Graybiel, 1992; C. J. Wilson, 1987) resulting in specific localized areas of button formation (Kincaid, Zheng, & Wilson, 1998) and small cortical areas innervating the striatum in a discontinuous pattern with areas of denser innervation separated by areas of sparse innervation (L. L. Brown, Smith, & Goldbloom, 1998; Flaherty & Graybiel, 1991). We also considered the large reduction in the number of neurons from cortex to striatum to GPi (Bar-Gad & Bergman, 2001; Oorschot, 1996). These findings combined lead to striatal areas that are mostly specific for input from one cortical area alongside areas where there is overlap between inputs from two or more cortical areas (Takada et al., 2001) and which are here referred to as the associative striatum.

The gain of the synaptic connection from population A (presynaptic) to population B (postsynaptic) is denoted as $G_{A \rightarrow B}$, and the total synaptic input to population B is:

Pop. A	Pop. B	Pathway	Pattern	Gain
Cortex	Striatum	cog. → cog. •	(i,1) → (i,1)	1.0
		mot. → mot.	(i,1) → (i,1)	1.0
		ass. → ass.	(i,j) → (i,j)	1.0
		cog. → ass.	(i,1) → (i,*)	0.2
		mot. → ass.	(1,i) → (*,i)	0.2
	STN	cog. → cog.	(i,1) → (i,1)	1.0
		mot. → mot.	(1,i) → (1,i)	1.0
	Thalamus	cog. → cog.	(i,1) → (i,1)	0.1
		mot. → mot.	(1,i) → (1,i)	0.1
	Cortex	cog. → cog.	(i,1) → (*,1)	±0.5
		mot. → mot.	(1,i) → (1,*)	±0.5
		ass. → ass.	(i,j) → (*,*)	±0.5
		ass. → mot.	(*,i) → (1,i)	0.025
		ass. → cog.	(i,*) → (i,1)	0.01
		cog. → ass. •	(i,1) → (i,*)	0.025
		mot. → ass.	(1,i) → (*,i)	0.01
Striatum	GPi	cog. → cog.	(i,1) → (i,1)	-2.0
		mot. → mot.	(1,i) → (1,i)	-2.0
		ass. → cog.	(i,*) → (i,1)	-2.0
		ass. → mot.	(*,i) → (1,i)	-2.0
	STN	cog. → cog.	(i,1) → (i,1)	1.0
		mot. → mot.	(1,i) → (1,i)	1.0
	GPi	cog. → cog.	(i,1) → (i,1)	-1.0
		mot. → mot.	(1,i) → (1,i)	-1.0
Thalamus	Cortex	cog. → cog.	(i,1) → (i,1)	1.0
		mot. → mot.	(1,i) → (1,i)	1.0

Table 3. Connectivity gains and pattern between the different populations. For connectivity patterns, “*” means all. For example, $(1,i) \rightarrow (1,*)$ means one-to-all connectivity while $(1,i) \rightarrow (1,i)$ means one-to-one connectivity. Plastic pathways are indicated by a “•” symbol.

$$I_{syn}^B = G_{A \rightarrow B} \sum_A U_A$$

where A is the presynaptic assembly, B is the postsynaptic assembly, and U_A is the output of presynaptic assembly A . The gains for each pathway are shown in Table 3. Gains to the corresponding cognitive (motor) assembly are initially five times higher than to each receiving associative area. Re-convergence from cognitive (motor) and association areas of striatum to cognitive (motor) areas of GPi are evenly weighted.

Task encoding

At the trial start, assemblies in the cognitive cortex encoding the two cues, C_1 and C_2 , receive an external current (7Hz) and assemblies in the motor cortex encoding the two positions, M_1 and M_2 , receive a similar external current (7Hz). These activities are ambiguous since they could mean $[C_1/M_1, C_2/M_2]$ or $[C_1/M_2, C_2/M_1]$ (binding problem). This is the reason why the associative cortex encoding one of these two situations receives an external current (7Hz), $(C_1/M_1, C_2/M_2)$ that allows to bind a stimulus with a position (see Fig. 5). The decision of the model is decoded from the activity in the motor cortex *only*, i.e. independently of the activity in the cognitive cortex. If the model chooses a given cue but produces the wrong motor command, the cognitive choice will not be taken into account, and the final choice will be decoded from the motor command, even

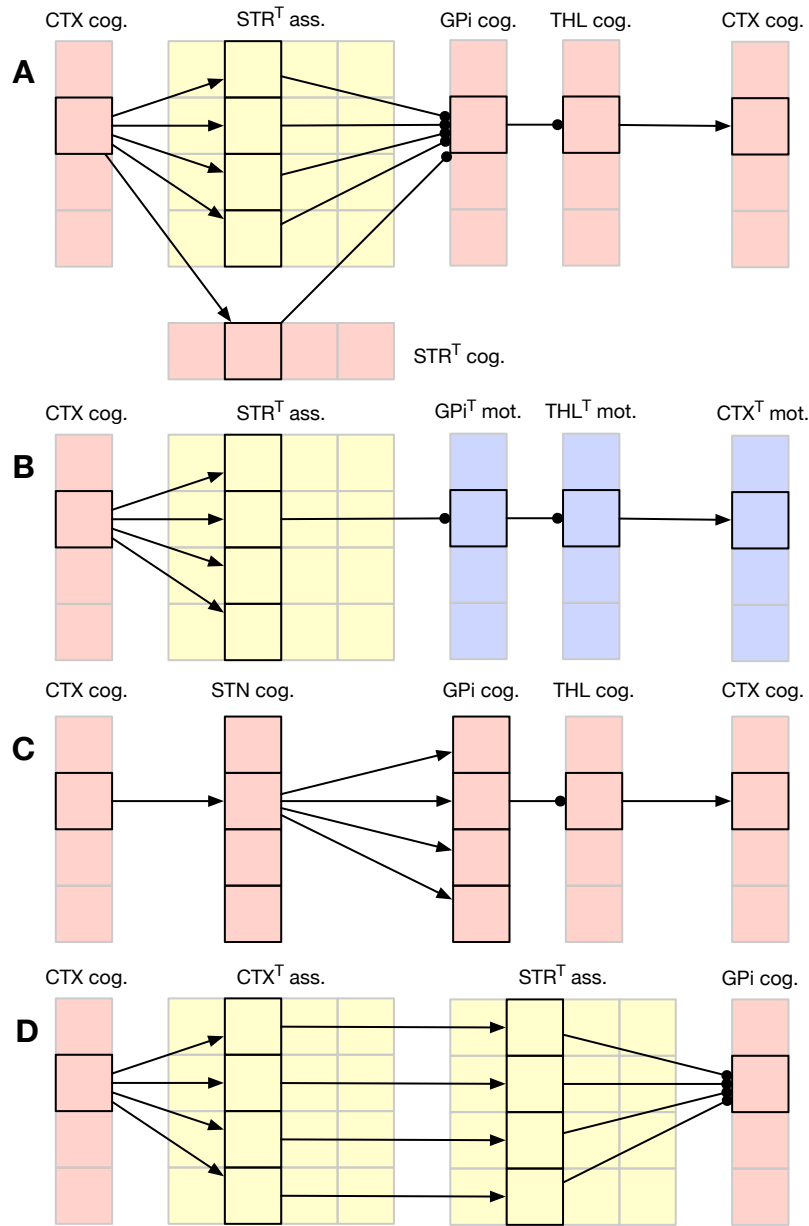


Figure 4. Partial connectivity in the cognitive and associative loops. For clarity, only one assembly has been considered. The motor loop is symmetric to the cognitive one. The “T” symbol on some name means the geometry of the group has been transposed (for readability). **A** The direct pathway from cognitive cortical assemblies diverge from cortex to associative and cognitive striatum. The pathway converges into cognitive GPi, send parallel projection to the thalamus and forms a closed loop with the original cognitive cortical assembly. **B** Thanks to the convergence of motor and cognitive pathways in associative striatum, there is a cross-talk between the motor and cognitive loops. This allows a decision to be made in the cognitive loop to influence the decision in motor loops and vice-versa. **C** The hyperdirect pathway from cognitive cortical assembly diverges from STN to GPi, innervating all cognitive, but not motor, GPi regions and feeds back to all cognitive cortical assemblies. **D** The pathway from associative cortex and associative striatum is made of parallel localized projections.

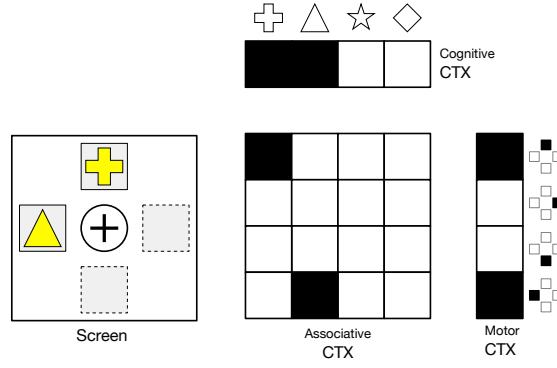


Figure 5. Task encoding. Assemblies in the cognitive cortex encoding the two cues, C_1 and C_2 , receive an external current, and assemblies in the motor cortex encoding the two positions, M_1 and M_2 , receive a similar external current. These activities are not sufficient to disambiguate between $[C_1/M_1, C_2/M_2]$ or $[C_1/M_2, C_2/M_1]$ (binding problem). This is the reason why the associative cortex encoding one of these two situations receives also an external current, $(C_1/M_1, C_2/M_2)$ in order to disambiguate the two cases, hence solving the binding problem.

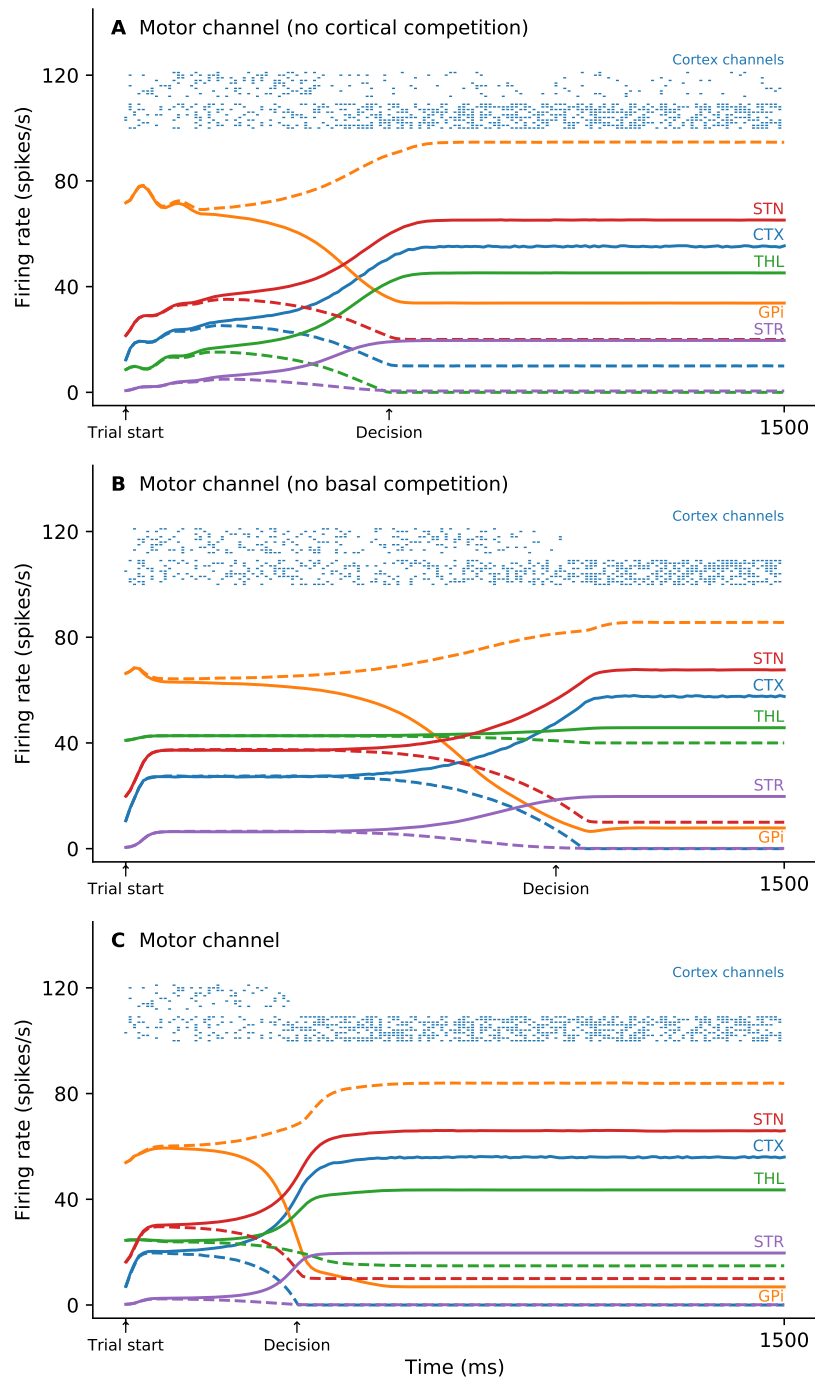
though that it may lead to an irrelevant choice.

Dynamics

Two different competition mechanisms exist inside the model. One is conveyed through the direct and hyperdirect pathways, the other is conveyed inside the cortex through short-range excitation and long range inhibition. The former has been fully described and analyzed in (Leblois et al., 2006) while the latter been extensively studied in a number of experimental and theoretical papers (Amari, 1977; Callaway, 1998; Taylor, 1999; von der Malsburg, 1973; H. R. Wilson & Cowan, 1972, 1973). Each of these two competition mechanisms can lead to a decision as illustrated on Fig. 6, which shows the dynamic of the motor loop for all the population in three conditions. In the absence of the cortical interactions (gain of cortical lateral connections has been set to 0), the direct and hyperdirect pathway are able to promote a competition that results in the selection of one of the two assemblies in each group. In the absence of GPi output (connection has been cut), the cortical lateral connections are able to support a competition resulting in the selection of one of the two assemblies, even though such decision is generally slower than decisions formed in the basal ganglia.. The result of the dual competition is a faster selection of one of the two assemblies after learning, when there is no possibility for the two competitions to be non congruent (one competition tends to select move A while the others tend to select move B). We will see in the results section that if the result of the two competitions is non-congruent, the decision is slower.

Learning

Learning has been restricted to the cognitive channel on the cortico-striatal synapse (between the cognitive cortex and striatum) and the cortico-cortical synapses (between the cognitive and associative cortex). Most probably there is learning in other structures and pathways, but the aim here is to show that the proposed restriction is sufficient to produce the behavior under consideration. All synaptic weights are initialized to 0.5 (SD 0.005) and used as a multiplier to the pathway gain in order to keep the factors of gain and weight separately observable. All weights are bound between W_{min} and W_{max} (see Table 4) such that for any change $\Delta W(t)$, weight $W(t)$ is updated according



to the equation:

$$W(t) \leftarrow W(t) + \Delta W(t)(W_{max} - W(t))(W(t) - W_{min})$$

Name	Value
W_{min}	0.25
W_{max}	0.75
LTP_{RL}	0.050
LTD_{RL}	0.030
LTP_{HL}	0.005
α	0.025

Table 4. Learning parameters

Reinforcement learning At the level of corticostriatal synapses, phasic changes in dopamine concentration have been shown to be necessary for the production of long-term potentiation (LTP) (Kerr & Wickens, 2001; Pawlak & Kerr, 2008; Reynolds, Hyland, & Wickens, 2001; Surmeier, Ding, Day, Wang, & Shen, 2007). After each trial, once reward has been received (0 or 1), the cortico-striatal weights are updated according to the reward prediction error (RPE):

$$\Delta W_B^A = LTP_{RL} \times RPE \times U_B \text{ if } RPE > 0 \quad (3)$$

$$= LTD_{RL} \times RPE \times U_B \text{ if } RPE < 0 \quad (4)$$

where ΔW_B^A is the change in the weight of the cortico-striatal synapse from cortical assembly A to striatal assembly B, RPE is the reward prediction error, the amount by which the actual reward delivered differs from the expected reward, U_B is the activation of the striatal assembly, and α is the actor learning rate. Generation of LTP and long-term depression (LTD) in striatal MSNs has been found to be asymmetric (Pawlak & Kerr, 2008). Therefore, in the model, the actor learning rate is different for LTP and LTD. The RPE is calculated using a simple critic learning algorithm:

$$RPE = R - V_i$$

where R , the reward, is 0 or 1, depending on whether a reward was given or not on that trial. Whether a reward was given, it was based on the reward probability of the selected cue (which is the one associated with the direction that was chosen). i is the number of the chosen cue, and V_i is the value of cue i . The value of the chosen cue is then updated using the RPE:

$$V_i \leftarrow V_i + \alpha RPE$$

Hebbian learning At the level of cortico-cortical synapses, only the co-activation of two assemblies is necessary for the production of long-term potentiation (Bear & Malenka, 1994; Caporale & Dan, 2008; Feldman, 2009; Hiratani & Fukai, 2016). After each trial, once a move has been initiated, the cortico-cortical weights are updated according to:

$$\Delta W_B^A = LTP_{HL} \times U_A \times U_B$$

where ΔW_B^A is the change in the weight of the cortico-cortical synapse from cognitive cortical assembly A to associative cortical assembly B. This learning rule is thus independent of reward.

Experimental setup

Experimental data were obtained from 2 female macaque monkeys (*Macaca mulata*). Experiments were performed during the daytime. Monkeys were living under a 12h/12h diurnal rhythm. Although food access was available ad libitum, the primates were kept under water restriction to increase their motivation to work. A veterinary skilled in healthcare and maintenance in nonhuman primates supervised all aspects of animal care. Experimental procedures were performed in accordance with the Council Directive of 20 October 2010 (2010/63/ UE) of the European Community. This project was approved by the French Ethic Committee for Animal Experimentation (50120111-A).

Surgical Procedure

Cannula guides were implanted into the left and right GPi in both animals under general anesthesia. Implantation was performed inside a stereotaxic frame guided by ventriculography and single-unit electrophysiological recordings. A ventriculographic cannula was introduced into the anterior horn of the lateral ventricle and a contrast medium was injected. Corrections in the position of the GPi were performed according to the line between the anterior commissure (AC) and the posterior commissure (PC) line. The theoretical target was AP: 23.0mm, L: 7.0 mm, P: 21.2 mm.²⁷ A linear 16-channel multielectrode array was lowered vertically into the brain. Extracellular single-unit activity was recorded from 0mm to 24 mm relative to the ACPC line with a wireless recording system. Penetration of the electrode array into the GPi was characterized by an increase in the background activity with the appearance of active neurons with a tonic firing rate (around the ACPC line). The exit of the electrode tips from the GPi was characterized by the absence of spike (around 3-4 mm below the ACPC line). When a clear GPi signal from at least 3 contacts had been obtained, control radiography of the position of the recording electrode was performed and compared to the expected position of the target according to the ventriculography. If the deviation from the expected target was less than 1mm, the electrode was removed and a cannula guide was inserted with a spare cannula inside so that the tip of the cannula was superimposed on the location of the electrode array in the control radiography. Once the cannula guide was satisfactorily placed, it was fixed to the skull with dental cement.

Bilateral Inactivation of the GPi

Micro-injections were delivered bilaterally 15 minutes before a session. For both animals' injections of the *GABA_A* agonist muscimol hydrobromide (Sigma) or saline (NaCl 9) were randomly assigned each day. Muscimol was delivered at a concentration of 1 μ g/ μ l (dissolved in a NaCl vehicle). Injections (1 μ l in each side) were performed at a constant flow rate of 0.2 μ l/min using a micro-injection system. Injections were made through a 30-gauge cannula inserted into the 2 guide cannula targeting left and right GPi. Cannulas were connected to a 25 μ l Hamilton syringe by polyethylene cannula tubing.

Data Analysis

Theoretical and experimental data were analyzed using Kruskal-Wallis rank sum test between the three conditions (saline (C0), muscimol (C1) or saline following muscimol (C2)) for the 6 samples (12 \times 10 first trials of C0 (control), 12 \times 10 last trials of C0 (control), 12 \times 10 first trials of C1 (GPi Off/muscimol); 12 \times 10 last trials of C1(GPi OFF/muscimol); 12 \times 10 first trials of C2(GPi On/saline); 12 \times 10 last trials of C2(GPi On/saline)) with posthoc pairwise comparisons using Dunn's-test for multiple comparisons of independent samples. P-values have been adjusted according to the false discovery rate (FDR) procedure of Benjamini-Hochberg. Results were obtained

from raw data using the PMCMR R package (Pohlert, 2014). Significance level was set at $P < 0.01$.

Experimental raw data is available from (Kase & Boraud, 2017) under a CC0 license, theoretical raw data and code are available from (Rougier & Topalidou, 2017) under a CC0 license (data) and BSD license (code). The data and the codes are also available as extended data (respectively model codes and experimental data files).

Results

Our model predicts that the evaluation of options and the behavioral outcome are two separate (but entangled) processes. This means that if we block the output of the basal ganglia before learning, reinforcement learning still occurs at the striatal level under dopaminergic control and should induce covert learning of stimuli value even though the behavioral choice would appear as random.

Protocol

The protocol has been consequently split over two consecutive conditions (C1 & C2) using the same set of stimuli and a dissociated control (C0) using a different set of stimuli (using same probabilities as for C1 & C2).

- C0 60 trials, GPi On (model), saline injection (primates),
stimulus set 1 (A_1, B_1) with $P_{A_1} = 0.75$, $P_{B_1} = 0.25$
- C1 60 trials, GPi Off (model), muscimol injection (primates),
stimulus set 2 (A_2, B_2) with $P_{A_2} = 0.75$, $P_{B_2} = 0.25$
- C2 60 trials, GPi On (model), saline injection (primates),
stimulus set 2 (A_2, B_2) with $P_{A_2} = 0.75$, $P_{B_2} = 0.25$

Computational results

H0	statistic (H)	p value
C0 start = C2 start	2.965	0.0051
C1 start = C2 start	4.986	1.8e-6
C1 end = C2 start	3.099	0.0036

Table 5. Theoretical results statistical analysis on correct answers. Kruskal-Wallis rank sum test between the three conditions (saline (C0), muscimol (C1) or saline following muscimol (C2)) with posthoc pairwise comparisons using Dunns-test for multiple comparisons of independent samples. The script used for the analysis (R language) is available from (Rougier & Topalidou, 2017).

We tested our hypothesis on the model using 12 different sessions (corresponding to 12 different initializations of the model). On day 1 (condition C1), we suppressed the GPi output by cutting the connections between the GPi and the thalamus. When the GPi output has been suppressed, the performance is random at the beginning, as shown by the average probability of choosing the best option (expressed in mean \pm SD) in the first 10 trials (0.408 ± 0.161), and remains so until the end of the session (0.525 ± 0.164). Statistical analysis revealed that no significant difference between the 10 first and 10 last trials. On day 2 (condition C2), we re-established the connections between GPi and thalamus, and tested the model to the same task as in C1 using the same set of stimuli. Results

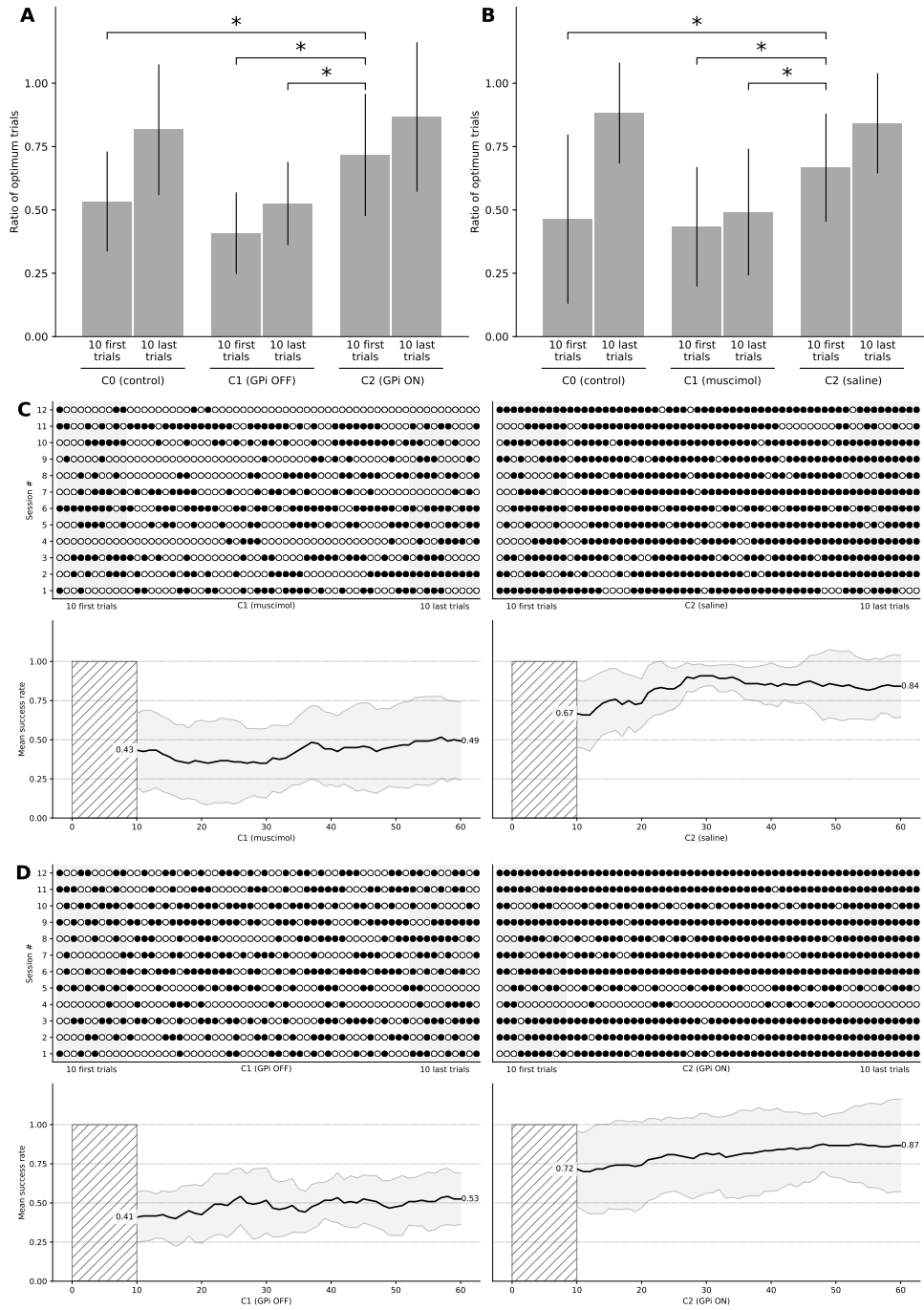


Figure 7. Theoretical and experimental results. Histograms show the mean performance at the start and the end of a session in C1 and C2 conditions for both the model (**A**) and the monkeys (**B**). At the start of C2, the performance for both the model and the monkeys is significantly higher compared to the start and end of C1, suggesting that covert learning has occurred during C1 even though performances are random during C1. **C** Individual trials ($n=2 \times 60$) for all the sessions ($n=12$) for the primates (monkey 1: sessions 1-7, monkey 2: sessions 8-12). **D** Individual trials ($n=2 \times 60$) for all the sessions ($n=12$) for the model. A black dot means a successful trial (the best stimulus has been chosen), an outlined white dot means a failed trial (the best stimulus has not been chosen). Measure of success is independent of the actual reward received after having chosen one of the two stimuli. The bottom part of each panel shows the mean success rate over a sliding window of ten consecutive trials and averaged across all the sessions. The thick black line is the actual mean and the gray-shaded area represents the standard deviation (STD) over sessions.

show a significant change in behavior: the model starts with an above-chance performance on the first 10 trials (0.717 ± 0.241) and this change is significant (see Table 5 and Fig. 7) compared to the start of C1, compared to the end of C1 and compared to the start of C0, confirming our hypothesis that the BG have previously learned the value of stimuli even though they were unable to alter the behavior of the model.

Experimental results

H0	statistic (H)	p value
C0 start = C2 start	3.181	0.0024
C1 start = C2 start	3.738	0.0004
C1 end = C2 start	2.803	0.0069

Table 6. Experimental results; statistical analysis on correct answers. Kruskal-Wallis rank sum test between the three conditions (saline (C0), muscimol (C1) or saline following muscimol (C2)) with posthoc pairwise comparisons using Dunns-test for multiple comparisons of independent samples. The script used for the analysis (R language) is available from (Rougier & Topalidou, 2017).

We tested the prediction of the model on two female macaque monkeys which have been implanted with two cannula guides into their left and right GPi (see Materials and Methods section for details). In order to inhibit the GPi, we injected bilaterally a GABA agonist (muscimol, $1\mu\text{g}$) 15 minutes before working session on day 1 (condition C1). The two monkeys were trained for 7 and 5 sessions respectively, using the same set of stimuli for each session. Results show that animals were unable to choose the best stimulus in such condition from the start (0.433 ± 0.236) to the end (0.492 ± 0.250) of the session. Statistical analysis revealed no significant difference between the 10 first and 10 last trials in C1. On day 2 (condition C2), we injected bilaterally a saline solution 15 minutes before working session, and animals had to perform the same protocol as in C1. Results show a significant change in behavior (see Table 6 and Fig. 7): animals start with an above-chance performance on the first 10 trials ($P=0.667 \pm 0.213$), compared to the start of C1, compared to the end of C1 and compared to the start of C0, confirming our hypothesis that the BG has previously learned the value of stimuli.

Discussion

Revisiting an old idea

The model architecture we proposed in this manuscript is not totally original in the sense that the model implements known pathways that have been established for quite a long time and taken into account in a number of models. More precisely, several computational models in the litterature include both the inner BG pathways as well as the feed-forward and feed-back loops from and to the cortex (through thalamus). However most of these models (if not all) put a specific emphasis on the role of the BG without considering the cortex as a decision making structure. To the best of our knowledge, virtually none of these models take advantage of a dual competition mechanism similar to the one we introduced. For example the model by O'Reilly and Frank (2006) that solves the temporal and structural credit assignment problems on a working memory task includes a Hebbian learning component for the posterior cortical part. However, authors shows that Hebbian learning is not critical for performances (only a 5% drop in performance) and did not specifically study lesions in the BG. Similarly, the model by (J. W. Brown, Bullock, & Grossberg, 2004) does include a laminar frontal part with a specific emphasis on the interaction between the BG and the frontal

cortex and explain how to balance between reactive and planned behaviors. However, authors considers that *lesions of the BG uniquely cause devastating disorders of the voluntary movement system* which is not always the case as we've shown with experimental data (Desmurget & Turner, 2010; Piron et al., 2016). The model by (Schroll, Vitay, & Hamker, 2013; Villagrasa et al., 2018) is notably similar to our own model and suggests that the cortico-basal ganglia pathway is not required to perform previously well-learned SR associations, which is quite consistent with our own hypothesis. By using a simple stimulus-response association tasks, authors show that a focal GPi lesion do not impact significantly performances over a previously well learned task. This is made possible thanks to the cortico-thalamic pathway that *learn to interconnect those cortical and thalamic neurons that are simultaneously activated via reward-sensitive BG pathways*. The main difference with our own model is the localisation of the Hebbian learning and the lateral competition. We hypothesize this learning to occur at the cortical level and take advantage of a lateral competition mechanism that is necessary to solve our decision task (while it is not necessary for a simple stimulus-response task). This lateral competition acts indeed as a Go/NoGo substitute in the absence of the BG output. Furthermore, authors did not specifically conclude on the presence of covert learning when GPi is lesioned. They showed that the model has very bad performance when learning a new task, but they did not test the model once GPi is unlesioned. We suspect that if they had tested it, they would have found results similar to our own.

Covert learning in the BG

These results reinforce the classical idea that the basal ganglia architecture is based on an actor critic architecture where the dopamine serves as a reinforcement signal. However, the proposed model goes beyond this classical hypothesis and proposes a more general view on the role of the BG in behavior and their entanglement with the cortex. Our results, both theoretical and experimental, suggest that the critic part of the BG extends its role beyond the basal ganglia and makes it *de facto* a central component in behavior that evaluates any action, independently of their origin. This hypothesis is very congruent with the results introduced in Charlesworth, Warren, and Brainard (2012) where authors show that the anterior forebrain pathway in Bengalese finches contributes to skill learning even when it is blocked and does not participate in the behavioral performance. This is also quite compatible with the hypothesis that the BG is a general purpose trainer for cortico-cortical connections as proposed by Ashby, Turner, and Horvitz (2010), H  lie, Ell, and Ashby (2015). Here, we introduced a precise computational model using both reinforcement and Hebbian learning, supported by experimental data, that explains precisely how this general purpose trainer can be biologically implemented.

This can be simply understood by scrutinizing a session in control and lesion condition (see Fig. 8). In control condition, the model learns to select the best cue thanks to the BG. Learning the best stimulus induces a preferential selection of the best stimulus in order to obtain a higher probability of reward. If the process is repeated over many trials, this leads implicitly to an over-representation of the more valuable stimuli at the cortical level and consequently, Hebbian learning will naturally reinforce this stimulus. In the lesion condition, selection is random and each stimulus is roughly selected with equal probability, which allows the BG to evaluate the two stimuli even more precisely. We believe this is the same for the monkeys even though we do not have access to internal values and weights. However, we can see on Fig. 9 that the estimated value of stimuli (computed as the probability of reward) reflects the highest value for the best stimulus. Similarly, the number of times a given stimulus has been selected is correlated with its actual value.

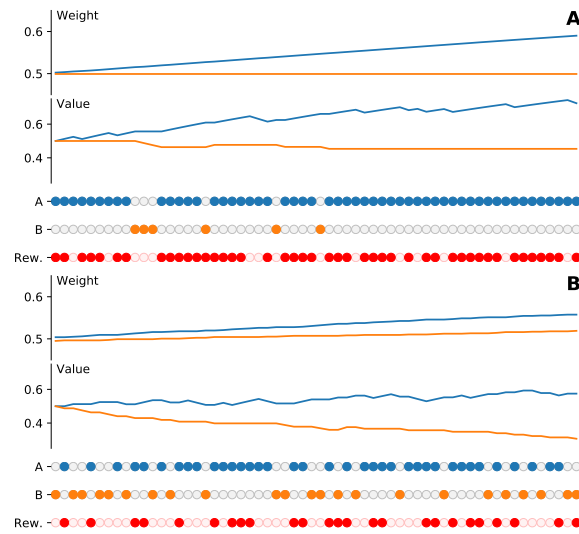


Figure 8. Model performance during a single session. Filled dots indicate the chosen cue between A and B. Filled red dots indicate if a reward has been received following the choice. Reward probability is 0.75 for cue A and 0.25 for cue B, but the displayed values are computed according to the actual reward received for each option. They are based on the history of the session, not the theoretical values. **A** Intact model (C0). The BG output drives the decision and evaluates the value of cue A and cue B with a strong bias in favor of A, because this cue is chosen more frequently. In the meantime, the Hebbian weight relative to this cue is strongly increased, while the weight relative to the other cue does not change significantly. **B** Lesioned model (C1). The BG output has been suppressed and decisions are random. Hebbian weights for cue A and cue B are both increased up to similar values at the end of the session. In the meantime, the value of cue A and cue B are evaluated within the BG and the random sampling of cue A and cue B leads to an actual better sampling of value A and B. This is clearly indicated by the estimated value of B that is very close to the theoretical value (0.25).

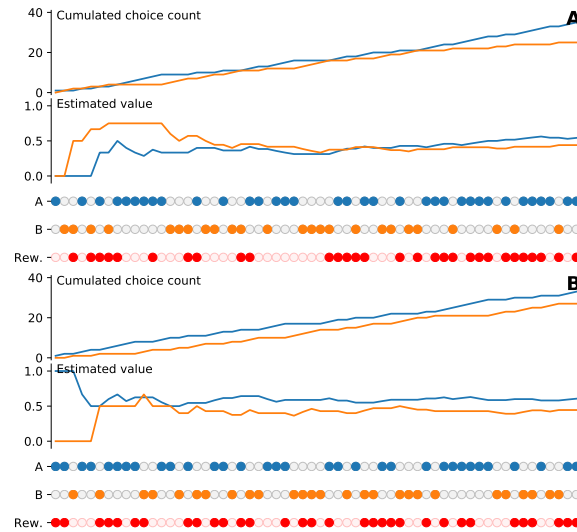


Figure 9. Monkey performance during a single session. Filled dots indicate the chosen cue between A and B. Filled red dots indicate if a reward has been received following the choice. Reward probability is 0.75 for cue A and 0.25 for cue B, but the displayed values are computed according to the actual reward received for each option. They are based on the history of the session, not the theoretical values. **A** In saline condition (C0), the monkey is able to slowly choose for the best cue with a slight preferences for A at the end of the 60 trials. Estimation of the perceived value of the two cues shows the actual value of A is greater than the value of B at the end of the session **B** In muscimol condition (C1), the monkey chooses cues randomly as indicated by the overall count of choices A and B. Estimation of the perceived value of the two cues (dashed lines) reveals a greater estimation of the value of A compared to the value of B.

From Reinforcement to Hebbian learning

These new results, together with our previous results (Piron et al., 2016), shed light on a plausible neural mechanism responsible for the gradual mix between an action-outcome and a stimulus-response behavior. The novelty in our hypothesis is that there is no transfer *per se*. There is instead a joint combination of the two systems that act and learn together, and we tend to disagree with the hypothesis of a hierarchical system (Dezfouli & Balleine, 2013). In our case, the final behavioral decision results from a subtle balance between the two decisions. When a new task needs to be solved, the basal ganglia initially drives the decision because initially it has a faster dynamic. In the meantime, the cortex takes advantage of this driving, and gradually learns the decision independently of the reward. We've shown how this could be the case for monkeys, even though we lack experimental evidence that the decision in muscimol condition is actually driven by the cortex. The actual combination of the two systems might be more complex than a simple weighted linear combination and this make the study even more difficult to carry on. What we see at the experimental level might be the projection of a more complex phenomenon. Persisting in a devaluated task does not mean that the system is *frozen*, but the time to come back from a stimulus-response oriented behavior might be simply longer than the time to initially acquire the behavior.

References

Alexander, G. E., & Crutcher, M. D. (1990). Functional architecture of basal ganglia circuits: Neural substrates of parallel processing. *Trends in neurosciences*. doi:10.1016/0166-2236(90)90107-L

- Alexander, G. E., Crutcher, M. D., & DeLong, M. R. (1991). Chapter 6 basal ganglia-thalamocortical circuits: Parallel substrates for motor, oculomotor, prefrontal and limbic functions. In *Progress in brain research* (pp. 119–146). doi:[10.1016/s0079-6123\(08\)62678-3](https://doi.org/10.1016/s0079-6123(08)62678-3)
- Alexander, G. E., DeLong, M. R., & Strick, P. L. (1986). Parallel organization of functionally segregated circuits linking basal ganglia and cortex. *Annual Review of Neuroscience*, 9(1), 357–381. doi:[10.1146/annurev.ne.09.030186.002041](https://doi.org/10.1146/annurev.ne.09.030186.002041)
- Amari, S.-i. (1977). Dynamics of pattern formation in lateral-inhibition type neural fields. *Biological Cybernetics*, 27(2), 77–87. doi:[10.1007/bf00337259](https://doi.org/10.1007/bf00337259)
- Ashby, F. G., Turner, B. O., & Horvitz, J. C. (2010). Cortical and basal ganglia contributions to habit learning and automaticity. *Trends in Cognitive Sciences*, 14(5), 208–215. doi:[10.1016/j.tics.2010.02.001](https://doi.org/10.1016/j.tics.2010.02.001)
- Auer, P., Cesa-Bianchi, N., Freund, Y., & Schapire, R. E. (2002). The nonstochastic multiarmed bandit problem. *SIAM Journal on Computing*, 32(1), 48–77. doi:[10.1137/S0097539701398375](https://doi.org/10.1137/S0097539701398375)
- Bar-Gad, I., & Bergman, H. (2001). Stepping out of the box: Information processing in the neural networks of the basal ganglia. *Current Opinion in Neurobiology*, 11(6), 689–695. doi:[10.1016/s0959-4388\(01\)00270-7](https://doi.org/10.1016/s0959-4388(01)00270-7)
- Bear, M. F., & Malenka, R. C. (1994). Synaptic plasticity: LTP and LTD. *Current Opinion in Neurobiology*, 4(3), 389–399. doi:[10.1016/0959-4388\(94\)90101-5](https://doi.org/10.1016/0959-4388(94)90101-5)
- Bradshaw, C. M., Szabadi, E., Bevan, P., & Ruddle, H. V. (1979). The effect of signaled reinforcement availability on concurrent performances in humans. *Journal of the Experimental Analysis of Behavior*, 32(1), 65–74. doi:[10.1901/jeab.1979.32-65](https://doi.org/10.1901/jeab.1979.32-65)
- Brown, J. W., Bullock, D., & Grossberg, S. (2004). How laminar frontal cortex and basal ganglia circuits interact to control planned and reactive saccades. *Neural Networks*, 17(4), 471–510. doi:[10.1016/j.neunet.2003.08.006](https://doi.org/10.1016/j.neunet.2003.08.006)
- Brown, L. L., Smith, D. M., & Goldbloom, L. M. (1998). Organizing principles of cortical integration in the rat neostriatum: Corticostriate map of the body surface is an ordered lattice of curved laminae and radial points. *The Journal of Comparative Neurology*, 392(4), 468–488. doi:[10.1002/\(SICI\)1096-9861\(19980323\)392:4<468::AID-CNE5>3.0.CO;2-Z](https://doi.org/10.1002/(SICI)1096-9861(19980323)392:4<468::AID-CNE5>3.0.CO;2-Z)
- Callaway, E. M. (1998). Local circuits in primary visual cortex of the macaque monkey. *Annual Review of Neuroscience*, 21(1), 47–74. doi:[10.1146/annurev.neuro.21.1.47](https://doi.org/10.1146/annurev.neuro.21.1.47)
- Caporale, N., & Dan, Y. (2008). Spike timing-dependent plasticity: A hebbian learning rule. *Annual Review of Neuroscience*, 31(1), 25–46. doi:[10.1146/annurev.neuro.31.060407.125639](https://doi.org/10.1146/annurev.neuro.31.060407.125639)
- Charlesworth, J. D., Warren, T. L., & Brainard, M. S. (2012). Covert skill learning in a cortical-basal ganglia circuit. *Nature*, 486(7402), 251–255.
- Coultrip, R., Granger, R., & Lynch, G. (1992). A cortical model of winner-take-all competition via lateral inhibition. *Neural Networks*, 5(1), 47–54. doi:[10.1016/s0893-6080\(05\)80006-1](https://doi.org/10.1016/s0893-6080(05)80006-1)
- Cowan, R. L., & Wilson, C. J. (1994). Spontaneous firing patterns and axonal projections of single corticostriatal neurons in the rat medial agranular cortex. *Journal of Neurophysiology*, 71(1), 17–32.
- Deco, G., Ponce-Alvarez, A., Hagmann, P., Romani, G. L., Mantini, D., & Corbetta, M. (2014). How local excitation-inhibition ratio impacts the whole brain dynamics. *Journal of Neuroscience*, 34(23), 7886–7898. doi:[10.1523/jneurosci.5068-13.2014](https://doi.org/10.1523/jneurosci.5068-13.2014)
- Desmurget, M., & Turner, R. S. (2010). Motor sequences and the basal ganglia: Kinematics, not habits. *Journal of Neuroscience*, 30(22), 7685–7690. doi:[10.1523/jneurosci.0163-10.2010](https://doi.org/10.1523/jneurosci.0163-10.2010)
- Dezfouli, A., & Balleine, B. W. (2013). Actions, action sequences and habits: Evidence that goal-directed and habitual action control are hierarchically organized. *PLoS Computational Biology*, 9(12), e1003364. doi:[10.1371/journal.pcbi.1003364](https://doi.org/10.1371/journal.pcbi.1003364)
- Doll, Bradley B, Simon, Dylan A, & Daw, Nathaniel D. (2012). The ubiquity of model-based reinforcement learning. *Current Opinion in Neurobiology*, 22(6), 1075–1081.
- Dougan, J. D., McSweeney, F. K., & Farmer, V. A. (1985). Some parameters of behavioral contrast and allocation of interim behavior in rats. *Journal of the Experimental Analysis of Behavior*, 44(3), 325–335. doi:[10.1901/jeab.1985.44-325](https://doi.org/10.1901/jeab.1985.44-325)
- Doya, K. (2000). Complementary roles of basal ganglia and cerebellum in learning and motor control. *Current Opinion in Neurobiology*, 10(6), 732–739.
- Doya, K. (2007). Reinforcement learning: Computational theory and biological mechanisms. *HFSP Journal*, 1(1), 30–11.
- Feldman, D. E. (2009). Synaptic mechanisms for plasticity in neocortex. *Annual Review of Neuroscience*, 32(1), 33–55. doi:[10.1146/annurev.neuro.051508.135516](https://doi.org/10.1146/annurev.neuro.051508.135516)
- Flaherty, A. W., & Graybiel, A. M. (1991). Corticostriatal transformations in the primate somatosensory system. projections from physiologically mapped body-part representations. *Journal of Neurophysiology*, 66(4), 1249–1263.
- Frank, M. J. [M. J.]. (2004). By carrot or by stick: Cognitive reinforcement learning in parkinsonism. *Science*, 306(5703), 1940–1943. doi:[10.1126/science.1102941](https://doi.org/10.1126/science.1102941)
- Gilbert-Norton, L. B., Shahan, T. A., & Shivik, J. A. (2009). Coyotes (canis latrans) and the matching law. *Behavioural Processes*, 82(2), 178–183. doi:[10.1016/j.beproc.2009.06.005](https://doi.org/10.1016/j.beproc.2009.06.005)

- Gittins, J. C. (1979). Bandit processes and dynamic allocation indices. *Journal of the Royal Statistical Society. Series B (Methodological)*, 41(2), 148–177.
- Glimcher, P. W. (2011). Understanding dopamine and reinforcement learning: the dopamine reward prediction error hypothesis. *Proceedings of the National Academy of Sciences*, 108 Suppl 3(Supplement 3), 15647–15654.
- Graft, D. A., Lea, S. E. G., & Whitworth, T. L. (1977). The matching law in and within groups of rats1. *Journal of the Experimental Analysis of Behavior*, 27(1), 183–194. doi:10.1901/jeab.1977.27-183
- Graybiel, A. M. (2008). Habits, rituals, and the evaluative brain. *Annual Review of Neuroscience*, 31(1), 359–387. doi:10.1146/annurev.neuro.29.051605.112851
- Graybiel, A. M., Aosaki, T., Flaherty, A. W., & Kimura, M. (1994). The basal ganglia and adaptive motor control. *Science*, 265(5180), 1826–1831. doi:10.1126/science.8091209
- Gurney, K., Prescott, T. J., & Redgrave, P. (2001). A computational model of action selection in the basal ganglia. II. analysis and simulation of behaviour. *Biological Cybernetics*, 84(6), 411–423. doi:10.1007/pl00007985
- Guthrie, M., Leblois, A., Garenne, A., & Boraud, T. (2013). Interaction between cognitive and motor cortico-basal ganglia loops during decision making: A computational study. *Journal of Neurophysiology*, 109, 3025–3040. doi:10.1152/jn.00026.2013
- Haber, S. N. (2003). The primate basal ganglia: Parallel and integrative networks. *Journal of Chemical Neuroanatomy*, 26(4), 317–330. doi:10.1016/j.jchemneu.2003.10.003
- Hélie, S., Ell, S. W., & Ashby, F. G. (2015). Learning robust cortico-cortical associations with the basal ganglia: An integrative review. *Cortex*, 64, 123–135. doi:10.1016/j.cortex.2014.10.011
- Herrnstein, R. J. (1974). Formal properties of the matching law1. *Journal of the Experimental Analysis of Behavior*, 21(1), 159–164. doi:10.1901/jeab.1974.21-159
- Herrnstein, R. J., Vaughan, W., Mumford, D. B., & Kosslyn, S. M. (1989). Teaching pigeons an abstract relational rule: Insideness. *Perception & Psychophysics*, 46(1), 56–64. doi:10.3758/bf03208074
- Hiratani, N., & Fukai, T. (2016). Hebbian wiring plasticity generates efficient network structures for robust inference with synaptic weight plasticity. *Frontiers in Neural Circuits*, 10. doi:10.3389/fncir.2016.00041
- Hopfield, J. J. (1984). Neurons with graded response have collective computational properties like those of two-state neurons. *Proceedings of the National Academy of Sciences*, 81(10), 3088–3092.
- Kase, D., & Boraud, T. (2017). Covert learning in the basal ganglia: Raw data. FigShare. doi:10.6084/m9.figshare.4753507.v1
- Katehakis, M. N., & Veinott, A. F. (1987). The multi-armed bandit problem: Decomposition and computation. *Mathematics of Operations Research*, 12(2), 262–268. doi:10.1287/moor.12.2.262
- Keasar, T. (2002). Bees in two-armed bandit situations: Foraging choices and possible decision mechanisms. *Behavioral Ecology*, 13(6), 757–765. doi:10.1093/beheco/13.6.757
- Kerr, J. N. D., & Wickens, J. R. (2001). Dopamine d-1/d-5 receptor activation is required for long-term potentiation in the rat neostriatum in vitro. *Journal of Neurophysiology*, 85(1), 117–124.
- Kincaid, A. E., Zheng, T., & Wilson, C. J. (1998). Connectivity and convergence of single corticostriatal axons. *Journal of Neuroscience*, 18(12), 4722–4731.
- Lau, B., & Glimcher, P. W. (2005). Dynamic response-by-response models of matching behavior in rhesus monkeys. *Journal of the Experimental Analysis of Behavior*, 84(3), 555–579. doi:10.1901/jeab.2005.110-04
- Lau, B., & Glimcher, P. W. (2008). Value representations in the primate striatum during matching behavior. *Neuron*, 58(3), 451–463. doi:10.1016/j.neuron.2008.02.021
- Leblois, A., Boraud, T., Meissner, W., Bergman, H., & Hansel, D. (2006). Competition between feedback loops underlies normal and pathological dynamics in the basal ganglia. *Journal of Neurosciences*, 26, 3567–3583. doi:10.1523/JNEUROSCI.5050-05.2006
- Matthews, L. R., & Temple, W. (1979). Concurrent schedule assessment of food preference in cows. *Journal of the Experimental Analysis of Behavior*, 32(2), 245–254. doi:10.1901/jeab.1979.32-245
- Mink, J. W. (1996). The basal ganglia: Focused selection and inhibition of competing motor programs. *Progress in Neurobiology*, 50(4), 381–425. doi:10.1016/S0301-0082(96)00042-1
- Mishkin, M., Malamut, B., & Bachevalier, J. (1984). Memories and habits: Two neural systems. In G. Lynch, J. L. McGaugh, & N. M. Weinberger (Eds.), *Neurobiology of human learning and memory*.
- Muir, D. R., & Cook, M. (2014). Anatomical constraints on lateral competition in columnar cortical architectures. *Neural Computation*, 26(8), 1624–1666. doi:10.1162/neco_a_00613
- Naruse, M., Berthel, M., Drezet, A., Huant, S., Aono, M., Hori, H., & Kim, S.-J. (2015). Single-photon decision maker. *Scientific Reports*, 5(1). doi:10.1038/srep13253
- Nisenbaum, E. S., & Wilson, C. J. (1995). Potassium currents responsible for inward and outward rectification in rat neostriatal spiny projection neurons. *Journal of Neuroscience*, 15(6), 4449–4463.
- Niv, Yael, & Langdon, Angela. (2016). Reinforcement learning with Marr. *Current Opinion in Behavioral Sciences*, 11, 67–73.
- O'Reilly, R. C., & Frank, M. J. [Michael J.]. (2006). Making working memory work: A computational model of learning in the prefrontal cortex and basal ganglia. *Neural Computation*, 18(2), 283–328. doi:10.1162/089976606775093909

- Oorschot, D. E. (1996). Total number of neurons in the neostriatal, pallidal, subthalamic, and substantia nigral nuclei of the rat basal ganglia: A stereological study using the cavalieri and optical disector methods. *The Journal of Comparative Neurology*, 366(4), 580–599. doi:[10.1002/\(SICI\)1096-9861\(19960318\)366:4<580::AID-CNE3>3.0.CO;2-0](https://doi.org/10.1002/(SICI)1096-9861(19960318)366:4<580::AID-CNE3>3.0.CO;2-0)
- Packard, M. G., & Knowlton, B. J. (2002). Learning and memory functions of the basal ganglia. *Annual Review of Neuroscience*, 25(1), 563–593. doi:[10.1146/annurev.neuro.25.112701.142937](https://doi.org/10.1146/annurev.neuro.25.112701.142937)
- Parent, A., Sato, F., Wu, Y., Gauthier, J., Lévesque, M., & Parent, M. (2000). Organization of the basal ganglia: The importance of axonal collateralization. *Trends in Neurosciences*, 23, S20–S27. doi:[10.1016/s1471-1931\(00\)00022-7](https://doi.org/10.1016/s1471-1931(00)00022-7)
- Parthasarathy, H., Schall, J., & Graybiel, A. M. (1992). Distributed but convergent ordering of corticostriatal projections: Analysis of the frontal eye field and the supplementary eye field in the macaque monkey. *Journal of Neuroscience*, 12(11), 4468–4488.
- Pasquereau, B., Nadjar, A., Arkadir, D., Bezard, E., Goillandeau, M., Bioulac, B., Gross, C. E., & Boraud, T. (2007). Shaping of motor responses by incentive values through the basal ganglia. *Journal of Neuroscience*, 27(5), 1176–1183. doi:[10.1523/jneurosci.3745-06.2007](https://doi.org/10.1523/jneurosci.3745-06.2007)
- Pawlak, V., & Kerr, J. N. D. (2008). Dopamine receptor activation is required for corticostriatal spike-timing-dependent plasticity. *Journal of Neuroscience*, 28(10), 2435–2446. doi:[10.1523/jneurosci.4402-07.2008](https://doi.org/10.1523/jneurosci.4402-07.2008)
- Piron, C., Kase, D., Topalidou, M., Goillandeau, M., Orignac, H., N'Guyen, T.-H., Rougier, N. P., & Boraud, T. (2016). The globus pallidus pars interna in goal-oriented and routine behaviors: Resolving a long-standing paradox. *Movement Disorders*, 31(8), 1146–1154. doi:[10.1002/mds.26542](https://doi.org/10.1002/mds.26542)
- Plowright, C., & Shettleworth, S. J. (1990). The role of shifting in choice behavior of pigeons on a two-armed bandit. *Behavioural Processes*, 21(2-3), 157–178. doi:[10.1016/0376-6357\(90\)90022-8](https://doi.org/10.1016/0376-6357(90)90022-8)
- Pohlert, T. (2014). *The pairwise multiple comparison of mean ranks package (pmmr)*. R Package. Retrieved from <http://CRAN.R-project.org/package=PMCMR>
- Redgrave, Peter, Gurney, Kevin, & Reynolds, John. (2008). What is reinforced by phasic dopamine signals? *Brain Research Reviews*, 58(2), 322–339.
- Reid, C. R., MacDonald, H., Mann, R. P., Marshall, J. A. R., Latty, T., & Garnier, S. (2016). Decision-making without a brain: How an amoeboid organism solves the two-armed bandit. *Journal of The Royal Society Interface*, 13(119), 20160030. doi:[10.1098/rsif.2016.0030](https://doi.org/10.1098/rsif.2016.0030)
- Reynolds, J. N. J., Hyland, B. I., & Wickens, J. R. (2001). A cellular mechanism of reward-related learning. *Nature*, 413(6851), 67–70. doi:[10.1038/35092560](https://doi.org/10.1038/35092560)
- Robbins, H. (1952). Some aspects of the sequential design of experiments. *Bulletin of the American Mathematical Society*, 58(5), 527–536. doi:[10.1090/s0002-9904-1952-09620-8](https://doi.org/10.1090/s0002-9904-1952-09620-8)
- Rougier, N. P., & Topalidou, M. (2017). Covert learning in the basal ganglia: Code. doi:[10.5281/zenodo.598112](https://doi.org/10.5281/zenodo.598112)
- Sandstrom, M. I., & Rebec, G. V. (2002). Characterization of striatal activity in conscious rats: Contribution of NMDA and AMPA/kainate receptors to both spontaneous and glutamate-driven firing. *Synapse*, 47(2), 91–100. doi:[10.1002/syn.10142](https://doi.org/10.1002/syn.10142)
- Schroll, H., Vitay, J., & Hamker, F. H. (2013). Dysfunctional and compensatory synaptic plasticity in parkinson's disease. *European Journal of Neuroscience*, 39(4), 688–702. doi:[10.1111/ejn.12434](https://doi.org/10.1111/ejn.12434)
- Seeger, C. A., & Spiering, B. J. (2011). A critical review of habit learning and the basal ganglia. *Frontiers in Systems Neuroscience*, 5. doi:[10.3389/fnsys.2011.00066](https://doi.org/10.3389/fnsys.2011.00066)
- Shriki, O., Hansel, D., & Sompolinsky, H. (2003). Rate models for conductance-based cortical neuronal networks. *Neural Computation*, 15(8), 1809–1841. doi:[10.1162/08997660360675053](https://doi.org/10.1162/08997660360675053)
- Steyvers, M., Lee, M. D., & Wagenmakers, E.-J. (2009). A bayesian analysis of human decision-making on bandit problems. *Journal of Mathematical Psychology*, 53(3), 168–179. doi:[10.1016/j.jmp.2008.11.002](https://doi.org/10.1016/j.jmp.2008.11.002)
- Suri, R. E., & Schultz, W. (1999). A neural network model with dopamine-like reinforcement signal that learns a spatial delayed response task. *Neuroscience*, 91(3), 871–890.
- Suri, R. E. (2002). TD models of reward predictive responses in dopamine neurons. *Neural Networks*, 15(4-6), 523–533.
- Surmeier, D. J., Ding, J., Day, M., Wang, Z., & Shen, W. (2007). D1 and d2 dopamine-receptor modulation of striatal glutamatergic signaling in striatal medium spiny neurons. *Trends in Neurosciences*, 30(5), 228–235. doi:[10.1016/j.tins.2007.03.008](https://doi.org/10.1016/j.tins.2007.03.008)
- Sutton, R. S., & Barto, A. G. (1998). *Reinforcement learning: An introduction*.
- Takada, M., Tokuno, H., Hamada, I., Inase, M., Ito, Y., Imanishi, M., Hasegawa, N., Akazawa, T., Hatanaka, N., & Nambu, A. (2001). Organization of inputs from cingulate motor areas to basal ganglia in macaque monkey. *European Journal of Neuroscience*, 14(10), 1633–1650. doi:[10.1046/j.0953-816x.2001.01789.x](https://doi.org/10.1046/j.0953-816x.2001.01789.x)
- Taylor, J. G. (1999). Neural 'bubble' dynamics in two dimensions: Foundations. *Biological Cybernetics*, 80(6), 393–409. doi:[10.1007/s004220050534](https://doi.org/10.1007/s004220050534)
- Villagrasa, F., Baladron, J., Vitay, J., Schroll, H., Antzoulatos, E. G., Miller, E. K., & Hamker, F. H. (2018). On the role of cortex-basal ganglia interactions for category learning: A neurocomputational approach. *The Journal of Neuroscience*, 38(44), 9551–9562. doi:[10.1523/jneurosci.0874-18.2018](https://doi.org/10.1523/jneurosci.0874-18.2018)

- von der Malsburg, C. (1973). Self-organization of orientation sensitive cells in the striate cortex. *Kybernetik*, 14(2), 85–100. doi:[10.1007/bf00288907](https://doi.org/10.1007/bf00288907)
- Webster, K. (1961). Cortico-striate interrelations in the albino rat. *Journal of anatomy*, 95, 532–544.
- Wilson, C. J. (1987). Morphology and synaptic connections of crossed corticostriatal neurons in the rat. *The Journal of Comparative Neurology*, 263(4), 567–580. doi:[10.1002/cne.902630408](https://doi.org/10.1002/cne.902630408)
- Wilson, C. J., & Groves, P. M. (1981). Spontaneous firing patterns of identified spiny neurons in the rat neostriatum. *Brain Research*, 220(1), 67–80. doi:[10.1016/0006-8993\(81\)90211-0](https://doi.org/10.1016/0006-8993(81)90211-0)
- Wilson, H. R., & Cowan, J. D. (1972). Excitatory and inhibitory interactions in localized populations of model neurons. *Biophysical Journal*, 12(1), 1–24. doi:[10.1016/s0006-3495\(72\)86068-5](https://doi.org/10.1016/s0006-3495(72)86068-5)
- Wilson, H. R., & Cowan, J. D. (1973). A mathematical theory of the functional dynamics of cortical and thalamic nervous tissue. *Kybernetik*, 13(2), 55–80. doi:[10.1007/bf00288786](https://doi.org/10.1007/bf00288786)
- Yin, H. H., & Knowlton, B. J. (2006). The role of the basal ganglia in habit formation. *Nature Reviews Neuroscience*, 7(6), 464–476. doi:[10.1038/nrn1919](https://doi.org/10.1038/nrn1919)